Title

Characterization of *CYCLOIDEA*-like genes in controlling floral zygomorphy in the monocotyledon *Alstroemeria*

Authors

Yoichiro Hoshino[1,*], Toshiya Igarashi[1], Masumi Ohshima[1], Koichi Shinoda[2], Naho Murata[2], Akira Kanno[3] and Masaru Nakano[4]

Affiliations and addresses

[1] Field Science Center for Northern Biosphere, Hokkaido University, Kita 11, Nishi 10, Kita-Ku, Sapporo 060-0811, Japan

[2] NARO Hokkaido Agricultural Research Center, Hitsujigaoka 1, Toyohira-ku, Sapporo 062-8555, Japan

[3] Graduate School of Life Sciences, Tohoku University, Katahira 2-1-1, Aoba-ku, Sendai 980-8577, Japan

[4] Faculty of Agriculture, Niigata University, 2-8050 Ikarashi, Niigata 950-2181, Japan

*Corresponding author: Yoichiro Hoshino

Field Science Center for Northern Biosphere, Hokkaido University, Kita 11, Nishi 10, Kita-Ku, Sapporo 060-0811, Japan

Telephone: +81-11-706-2857 FAX: +81-11-706-2857

E-mail: hoshino@fsc.hokudai.ac.jp

ABSTRACT

The *CYCLOIDEA* (*CYC*) gene controls the development of zygomorphic flowers and the determination of adaxial identity of floral organs in the model developmental system of *Antirrhinum majus*. However, whether *CYC* homologue genes also control floral zygomorphy in monocotyledon *Alstroemeria* plants is yet unknown. In this study, we investigated *CYC*-like genes in the monocotyledons *Alstroemeria aurea*, *A. magenta*, and *A. pelegrina* var. *rosea*, all of which have zygomorphic flowers. Since the *CYC* gene belongs to the T-complex protein (TCP) gene family of transcription factors, cloning of *CYC*-like sequences was performed using rapid amplification of cDNA ends (RACE)-polymerase chain reaction (PCR) by using degenerate primers designed for the TCP domain. We cloned 1 *CYC*-like sequence each from *A. aurea* (*AaTCP1*, accession number AB714967 in the GenBank/EMBL/DDBJ databases) and *A. magenta* (*AmTCP1*, AB714970), and 2 *CYC*-like sequences from *A. pelegrina* var. *rosea* (*ApTCP1*, AB714968; and *ApTCP2*, AB714969). The deduced amino acid sequences of *AaTCP1*, *AmTCP1*, *ApTCP1*, and *ApTCP2* shared 67.7%, 67.7%, 71.0%, and 64.5% identities, respectively, with the TCP domain in *CYC*. Molecular phylogenetic analysis indicated that 3 *CYC*-like genes from *Alstroemeria* belonged to the *ZinTBL1b* clade in the *CYC-/tb1*-like subfamily. Reverse transcription (RT)-PCR and *in situ* hybridization analyses showed that *AaTCP1* transcripts were specifically detected in flower buds and localized in the base of adaxial inner perianth of *A. aurea*. These results suggest that *CYC*-like genes are also involved in the development of floral asymmetry and the determination of adaxial identity of floral organs in the monocotyledon *Alstroemeria*.

Keywords: Alstroemeriaceae; *CYCLOIDEA*-like genes; floral asymmetry; monocotyledon; zygomorphy

Abbreviations: *CYC*, *CYCLOIDEA*; *DICH*, *DICHOTOMA*; RACE-PCR, Rapid amplification of cDNA ends-polymerase chain reaction; *Tb1*, *Teosinte branched 1*; TE, Tris-EDTA

1. Introduction

Zygomorphic flowers are thought to have evolved from radially symmetric flowers in response to the evolution of specialized pollinators, since their corollas (petal whorls) encourage an approach from one particular direction (Stebbins 1974; Endress, 1999). Thus far, the genetic mechanisms of floral zygomorphy have been studied in Ranunculales, Fabales, Brassicales, Lamiales, and Dipsacales (Jabbour et al., 2009). Endress (1999) and Stebbins (1974) indicated that zygomorphic flowers independently evolved in several clades in order to adapt to diverse pollination methods associated with specialized pollinators. This suggests that the occurrence of floral zygomorphy plays an important role in the diversification of flowering plants (Cubas, 2004; Citerne et al., 2010).

The genetic machinery for the occurrence of zygomorphic flowers was first identified in *Antirrhinum majus*, where it was found that the *CYCLOIDEA* (*CYC*) gene is required for the development of zygomorphic flowers and the determination of adaxial identity of floral organs (Luo et al., 1996; 1999). Both *CYC* and *DICHOTOMA* (*DICH*) are expressed in the adaxial region of the floral meristem of *A. majus*. The expression of the *CYC* and *DICH* genes is restricted in the adaxial region during petal and stamen formation (reviewed in Preston and Hileman, 2009). Coordination of expression patterns of these genes contributes to the determination of floral asymmetry.

The *CYC* gene belongs to the T-cell protein (TCP) gene family of transcription factors, which are characterized by a highly conserved DNA-binding region (Kosugi and Ohashi, 1997; 2002). This conserved region was named the TCP domain, which originated from *Teosinte branched 1* (*Tb1*) from *Zea mays* (Doebley et al., 1997),

CYC from *A. majus* (Luo et al., 1996), and *PROLIFERATING CELL FACTORS 1* and *2* (*PCF1* and *PCF2*) from *Oryza sativa* (Kosugi and Ohashi, 1997).

TCP gene family is divided to 2 major clades: Class I (PCF-like genes) and Class II (Kosugi and Ohashi, 1997; 2002; Cubas et al., 1999; Howarth and Donoghue, 2006; Martín-Trillo and Cubas, 2010). Class II comprises of *CYC-/tb1*- and *CIN*-like clades. By using degenerate primers designed for the TCP domain, researchers have cloned the *CYC* homologues from a wide range of eudicotyledonous plants belonging to the families Gesneriaceae (Citerne et al., 2000), Fabaceae (Fukuda et al., 2003; Citerne et al., 2006; Feng et al., 2006; Wang et al., 2008), Caprifoliaceae (Howarth et al., 2011), Fumariaceae (Kölsch and Gleissberg, 2006), Papaveraceae (Kölsch and Gleissberg, 2006), Solanaceae (Reeves and Olmstead, 2003), and Plantaginaceae (Baldwin et al., 2011), as well as from the model plant *Arabidopsis thaliana* (Cubas et al., 1999). Howarth and Donoghue (2006) analysed *CYC-/tb1* clade in eudicots and revealed the duplications during the evolutionary process. Two duplication events in *CYC-/tb1*-like genes were proposed to have led to the development of 3 subgroups, *CYC1*, *CYC2*, and *CYC3* (Howarth and Donoghue, 2006; Chapman et al., 2008).

Unlike the extensive studies in eudicots, the role of *CYC* genes for the establishment of floral zygomorphy in monocots has not been widely investigated (Mondragón-Palomino and Trontin, 2011). *CYC* research in monocotyledonous plants has been reported in graminaceous plants such as *Oryza sativa* (Kosugi and Ohashi, 1997; Yuan et al., 2009) and *Zea mays* (Doebley et al., 1997). Rudall and Bateman (2004) summarized patterns and processes that induced floral zygomorphy in monocots. Recently, Bartlett and Specht (2011) analysed *CYC* genes in Zingiberales (Costaceae and Heliconiaceae) and suggested that changes of expression pattern of *TB1*-like genes provide a mechanism for evolutionary shifts in floral zygomorphy.

Preston and Hileman (2012) also characterized *CYC* genes in *Commelina* and *Tradescantia* (Commelinaceae). Monocot *TCP*-like sequences were found to be associated in 20 major groups with an average identity of ≥64% and corresponded to well-supported clades of the phylogeny. In order to resolve the detailed common genetic machinery of floral zygomorphy in eudicotyledonous and monocotyledonous plants, further cloning and analysis of *CYC* homologue genes in monocotyledonous plants is required.

Plants belonging to the monocotyledonous genus *Alstroemeria*, family Alstroemeriaceae, have recently become popular as ornamentals, and thus are prized for their floral morphology. Furthermore, molecular mechanisms controlling flower development in this plant species have been studied by analysing class B genes (Hirai et al., 2007) and *LEAFY*-like gene (Hirai et al., 2012). Additionally, genetic transformation of *Alstroemeria* has been established by using *Agrobacterium tumefaciens* (Kim et al., 2007; Hoshino et al., 2008). These research findings will be useful for further analyses of flower development in this plant species. Therefore, in this study, we investigated *CYC* homologue genes in controlling floral symmetry in *Alstroemeria aurea*, *A. magenta*, and *A. pelegrina* var. *rosea*, all of which have zygomorphic flowers. The genus *Alstroemeria* contains 75 species (Hofreiter and Rodriguez, 2006), of which, these 3 species retain horticultural importance because of their high ornamental values (Fig. 1) and are considered to be the origins of present cultivars. Furthermore, flower characteristics of these species have been extensively evaluated (Kashihara et al., 2011). Therefore, these 3 species were selected for this study in order to establish a model for analysing floral zygomorphy in *Alstroemeria*. We cloned *CYC*-like genes from these plants and analysed their expression pattern by using reverse transcription polymerase chain reaction (RT-PCR). We then used *in situ*

hybridization to investigate the localization of *CYC*-like gene expression in the floral organs. Finally, we investigated how floral zygomorphy is related to *CYC*-like gene expression in *Alstroemeria*.

2. Materials and methods

2.1. Plant materials

Three species of *Alstroemeria* (*A. aurea*, *A. magenta*, and *A. pelegrina* var. *rosea*; Fig. 1) were used in the present study. Potted plants of each species were cultivated in a greenhouse at Experiment Farms, Field Science Center for Northern Biosphere, Hokkaido University, Japan. Plants were grown under natural light conditions, and the greenhouse was maintained at a minimum temperature of 15°C by heating during winter.

2.2. Extraction of total RNA

Total RNA was extracted from ca. 3–5-mm flower buds using the Concert Plant RNA Reagent (Invitrogen, San Francisco, CA, USA), following the manufacturer's instructions. Approximately 5 g fresh weight of flower buds was ground in liquid nitrogen, following which, 2 mL of Concert Plant RNA Reagent was added to the samples. Total RNA was then extracted according to the manufacturer's instructions, and purified RNA was dissolved in 100 μL of Tris-EDTA (TE) buffer. The concentration of extracted total RNA was measured using a spectrophotometer (ND-1000; Nano-Drop Technologies, Wilmington, DE, USA).

2.3. Cloning of *CYC* homologues

The total RNA extracted from flower buds was used as a template for PCR at a concentration of 5 $\mu g \cdot mL^{-1}$. Next, 1 μL of an adapter primer (10 mM) (5′-GGC CAC GCG TCG ACT AGT ACT_{17}) was mixed with 10 μL distilled water (DW). The samples were denatured by incubating for 10 min at 70°C and then quickly transferred onto ice. For the reverse transcriptase reaction, the reaction solution (2 μL 10× PCR buffer, 2 μL 25 mM $MgCl_2$, 1 μL 10 mM dNTP mix, 2 μL 0.1 M dithiothreitol (DTT); total 7 μL) was added to the template RNA, and the mixture was then incubated for 5 min at 42°C. Subsequently, 1 μL of the SuperScriptII reverse transcriptase (Gibco BRL; 200 $U \cdot \mu L^{-1}$) was added to the mixture, which was then incubated at 42°C for 50 min and at 70°C for 15 min. The first-strand cDNA obtained from this procedure was treated with 1 μL RNase H (2 $U \cdot \mu L^{-1}$) for 20 min at 37°C.

Three degenerate primers for the *CYC* homologue genes were constructed using previously published data [see Additional Information−Table 1] and used for PCR: TCP1 (5′-AAA GAY CGV CAC AGC AAR RTA), TCP2 (5′-CAC AGC AAR ATA TAC ACV BCM CAA), and R primer (5′-CTT CTC TTD GTT CKY TCC CT). PCR products were purified using the Wizard SV Gel and PCR Clean-Up System (Promega).

The PCR products were ligated with the pGEM-T Easy Vector (Promega) and used to transform competent cells of *Escherichia coli* XL1-Blue. Samples were incubated overnight, white colonies were selected, and PCR was performed using M13 primer M4 (5′-GTT TTC CCA GTC ACG AC) and M13 primer RV (5′-CAG GAA ACA GCT ATG AC).

The sequences obtained in this way from *A. aurea* were used for the construction of the specific primers 3′TCP-1 (5′-CGA TTT CTT CAA GCT CCA A) and 5′TCP-1 (5′-ACC TTT GCT CTA CAC TCC CTA). *ApTCP1* and *AmTCP1* were

then cloned from these primers. The PCR products were treated with a Dye Terminator Cycle Sequencing Kit (DTCS; Beckman Coulter) and analysed using an automatic sequencer (CEQ 8000; Beckman Coulter).

2.4. Phylogenetic analysis

Phylogenetic analysis of amino acid sequences of *CYC* homologue genes was performed using the programme SEAVIEW (Galtier et al., 1996). The amino acid sequences were aligned using TCP domain with the SEAVIEW, and a phylogenetic tree was constructed using the maximum likelihood (ML) method by using PhyML 3.0 program. Bootstrap analysis (100 replicates) was performed on the data set.

2.5. RT-PCR analysis for *CYC* homologue gene expression

Total RNA was extracted from *A. aurea* flower buds of different lengths (0.5−1, 1−2, and 2−3 mm longitudinal diameter), leaves, and stems. cDNA was synthesized from the total RNA using RT-PCR. The specific primers for *AaTCP1*, 3′TCP-1 (5′-CGA TTT CTT CAA GCT CCA A) and 5′TCP-1 (5′-ACC TTT GCT CTA CAC TCC CTA), were prepared. Pprimers specific to the actin gene of *A. aurea* [ACTIN-1 (5′-GTA TTG TGT TGG ACT CTG GTG ATG GTG T) and ACTIN-2 (5′-GAT GGA TCC TCC AAT CCA GAC ACT GTA)] were used as a control, on the basis of the assumption that different genes with the same transcript numbers will have equal PCR threshold cycle values. Amplification was carried out using an iCycler thermalcycler (Bio-Rad, Hercules, CA), with 1 cycle at 94°C for 5 min, and either 20, 25, or 35 cycles for 1 min at 94°C, 1 min at 55°C, and 1 min at 72°C in a 50 μL PCR solution, including 1 μL first-strand cDNA, 0.5 μL Ex Taq DNA polymerase (5 $U \cdot \mu L^{-1}$) (Takara), 5 μL 10× PCR buffer with $MgCl_2$, 4 μL 2.5 mM dNTP mix, 5 μL of each of

the primers, and 29.5 μL DW. Subsequently, gel electrophoresis of the PCR products was performed.

2.6. Histological *in situ* hybridization

Flower buds of *A. aurea* were fixed in FAA (50% formaldehyde, 5% acetic acid, 4% formaldehyde) and immediately aspirated for 40 min. The samples were then dehydrated in an ethanol series, and maintained in 99.5% ethanol overnight at 4°C. The samples were soaked several times in absolute ethanol and dehydrated completely in absolute ethanol for 20 min at room temperature. They were then passed through a graded tertiary butyl alcohol (TBA) series and embedded in paraffin (Paraplast Plus; Oxford Labware, St. Louis, USA).

Serial sections were cut at 10 μm by using a microtome (HM315; Carl Zeiss, Oberkochen, Germany) and placed on glass slides coated with APS (S8111, Matsunami Glass Ind., Ltd., Osaka, Japan). The slides were treated twice in xylene for 10 min, and passed through a graded ethanol series (2× absolute ethanol for 30 min, followed by 95%, 85%, 70%, 50%, and 30% ethanol for 30 s each). The slides were immersed in sterilized DW twice for 30 s and placed in 0.2 N HCl for 20 min. The slides were then immersed in a protease buffer containing 100 mM Tris-HCl (pH 7.5) and 50 mM EDTA (pH 8.0) and treated with RNase-free proteinase K (1 $mg \cdot mL^{-1}$ in protease buffer) for 30 min at 37°C. Next, the slides were immersed in sterilized DW for 5 min and passed through 0.1 M triethanolamine for 5 min (pH 8.0) twice, acetic anhydride (0.25% in 0.1 M triethanolamine) for 10 min, 2× SSC for 5 min, sterilized DW for 5 min, a graded ethanol series (30%, 50%, 75%, and 95% ethanol for 5 min each), and 99.5% ethanol for 5 min twice. The slides were dried under reduced pressure with an aspirator for 1 h.

For hybridization, 2 $mg \cdot mL^{-1}$ (final concentration) of a DIG-labelled probe was added to hybridization buffer consisting of 50% (v/v) formaldehyde, 300 mM NaCl, 10 mM Tris-HCl (pH 7.5), 1 mM EDTA (pH 8.0), 1× Denhardt (0.02% (w/v) Ficoll 400, 0.02% (w/v) polyvinylpyrrolidone, 0.02 (w/v) BSA, 0.25% SDS, 125 $mg \cdot mL^{-1}$ denatured DNA, 125 $mg \cdot mL^{-1}$ yeast RNA, and 10% (w/v) dextran sulphate. The probes were synthesized by PCR from the sequences for *AaTCP1* (348 bp). The probes were used as an antisense probe. Sense probe was also prepared and used as a control experiment. Each hybridization solution was added to each of the tissue sections, and the sections were incubated in a humidified box at 48°C for 12–16 h.

Following hybridization, sections were washed by electro-washing, according to the methods of Kobayashi et al. (1994). The hybridization signals were detected using anti-DIG conjugated with alkaline phosphatase and visualized with reaction buffer (100 mM Tris-HCl (pH 9.5), 100 mM NaCl, 5 mM $MgCl_2$, 0.2 mM nitroblue tetrazolium chloride, and 0.2 mM 5-bromo-4-chloro-3-indolyl-phosphate). Following visualization (2–3 h incubation), the sections were treated twice with a solution of 10 mM Tris-HCl (pH 7.5) and 1 mM EDTA for 5 min and covered in 70% glycerol with a coverslip. The slides were observed using a stereomicroscope (SMZ800, Nikon) and imaged using a digital camera (Digital Sight DS-L, Nikon).

3. Results

3.1. *CYC-like genes from* Alstroemeria

The deduced amino acid sequences of the cloned cDNAs *AaTCP1*, *AmTCP1*, *ApTCP1*, and *ApTCP2* were aligned with those of *CYC*, *DICHOTOMA* (*DICH*), *TB1*, *OsTB1*, and *TCP1* (Fig. 2). The deduced amino acid sequences shared 67.7%, 67.7%, 71.0%, and 64.5% identities, respectively, with the TCP domain in *CYC*, indicating that *CYC*-

like derived from *Alstroemeria* have high sequence similarity to other *CYC*-like genes (Fig. 2). *ApTCP1* and *AmTCP1* had very high similarity (approximately 93%) to the entire sequence of *CYC*, whereas *AaTCP1* and *ApTCP2* had considerably lower similarities (68.3% and 49.0%, respectively).

3.2. *Phylogenetic analysis*

TCP family genes have previously been separated into 2 subfamilies: Class I (*PCF*-like) and Class II (Kosugi and Ohashi, 1997, 2002; Cubas et al., 1999). Furthermore, Bartlett and Specht (2011) classified 8 clades of *ZinTBL1a*, *ZinTBL1b*, *ZinTBL2*, *PoaTBL1*, *PoaTBL2*, *CYC1*, *CYC2,* and *CYC3*. In the present study, the deduced amino acid sequences from the TCP domain of *AaTCP1*, *ApTCP1*, *AmTCP1*, and *ApTCP2* were aligned and analysed using the ML method (Fig. 3). This suggested that *AaTCP1*, *ApTCP,* and *AmTCP1* were located in *ZinTBL1b*. Amongst the *Alstroemeria* sequences in the present study, *ApTCP2* was separated from *AaTCP1*, *ApTCP1*, and *AmTCP1*. This indicated that *A. pelegrina* might have 2 types of *TCP* genes.

3.3. *Expression of AaTCP1 in* Alstroemeria aurea

In *A. aurea*, the specific band showing RNA expression of *AaTCP1* was observed in flower buds but not in leaves or stems (Fig. 4). When 3 developmental stages of flower buds (0.5–1, 1–2, and 2–3 mm) were analysed, the number of PCR cycles was found to affect the detection of *AaTCP1*: when 25 PCR cycles were run, *AaTCP1* was only detected in 2–3 mm flower buds, whereas 35 PCR cycles detected *AaTCP1* bands in all sizes of flower buds (Fig. 5). In contrast, *ACTIN*, which was used as the control, was detected in all samples under all conditions (Fig. 5). This indicates that *AaTCP1* is developmentally expressed in flower buds.

3.4. *Localization of* AaTCP1 *mRNA during flower development*

To identify the localization pattern of *AaTCP1* mRNA, transverse sections of flower buds of *A. aurea* were hybridized *in situ* with DIG-labelled sense or antisense *AaTCP1*. For samples that were hybridized with antisense probes, signals were detected in the adaxial inner perianth, gynoecium, and filaments of basal flower buds (Fig. 6). No signal was obtained from the samples that were hybridized with sense probes. Localization pattern of *AaTCP1* mRNA was examined in longitudinal sections (Fig. 7). The signals were observed in central portion of flower buds. Strong signals were localized in base of inner and outer perianth, filaments, anthers, and gynoecium. The localization patterns were similar to those of transverse sections shown in Fig. 6. These findings suggest that *AaTCP1* expression might be involved in flower formation, resulting in floral zygomorphy.

4. Discussion

Previous studies have investigated floral zygomorphy in *Antirrhinum majus* and the role of the *CYC* gene in controlling floral zygomorphy (Luo et al., 1996; Cubas et al., 1999). In the present study, we analysed floral zygomorphy in 3 species of the monocotyledon *Alstroemeria*. Conserved amino acid sequences from these genes were used to design degenerate primers, which were used to clone 4 *CYC*-like sequences (*AaTCP1*, *ApTCP1*, *ApTCP2*, and *AmTCP1*) using 5′RACE. Phylogenetic analysis was then performed on the deduced amino acid sequences of *AaTCP1*, *ApTCP1*, *ApTCP2*, and *AmTCP1* by using the ML method, which indicated that *AaTCP1*, *ApTCP1*, and *AmTCP1* were located in *ZinTBL1b* clade of the *CYC-/tb1-*

like subfamily, suggesting that these sequences have a high degree of similarity with other *CYC*-like genes.

Two clones (*ApTCP1* and *ApTCP2*) were isolated from *A. pelegrina* var. *rosea* in this study, indicating that gene duplication might have occurred at some time in the past. *ApTCP1* was more similar to *AaTCP1* and *AmTCP1* than to *ApTCP2*. *CYC* and *DICH* have been reported to have arisen from gene duplication in *A. majus* (Luo et al., 1999), and species closely related to *A. majus* have also been found to have *CYC* genes with gene duplication (Vieira et al. 1999). Gene duplication of *CYC* might be responsible for the development of the unique flower shape (papilionoid flowers) in plants belonging to Fabaceae (Fukuda et al., 2003). Gene duplication of *CYC* might also be related to floral evolution in monocotyledons such as *Alstroemeria*.

In *A. majus*, *CYC* is involved in petal and gynoecium development in the abaxial region of flower buds (Luo et al., 1996; 1999). To determine the temporal and spatial expression patterns of *CYC* homologue genes in *Alstroemeria*, we used RT-PCR and *in situ* hybridization to analyse the expression of *AaTCP1*. RT-PCR indicated that *AaTCP1* is expressed in flower buds but not in leaves or stems, and that during floral development, *AaTCP1* expression is enhanced and maintained in the late stage of flower bud formation. Previous studies have reported that *TCP1* expression disappears in late flower buds in *Arabidopsis* having symmetrical flowers (Cubas et al., 2001), while *CYC* expression is maintained throughout floral development in *A. majus* (Luo et al., 1996; 1999). This difference in expression patterns between symmetrical and actinomorphic flowers matches the pattern observed in this study for *Alstroemeria* plants with floral zygomorphy. The expression regions of *CYC* homologue genes in *Alstroemeria* were identified by hybridizing flower buds *in situ* using an antisense probe. Signals were observed at the inner perianth of the adaxial

region (Figs. 6 and 7). In *Lupinus nanus* (Fabaceae), *LegCYC1A* and *LegCYC1B* were also detected in similar floral tissue (Citerne et al., 2006). Hence, the *CYC* homologue gene expression in *A. aurea* might be involved in floral zygomorphy, as is involved in *A. majus* and *L. nanus*. This result suggests that the expression pattern of *CYC* homologue genes has been conserved between eudicot and monocot plants.

Alstroemeria flowers that possess specific spots on the perianth (Fig. 1e) and distinguishable perianth shapes are considered to be useful for the analysis of floral zygomorphy. Furthermore, an *Agrobacterium*-mediated transformation system has now been established in *Alstroemeria* (Kim et al., 2007; Hoshino et al., 2008). Thus, *Alstroemeria* will continue to be used in future studies to investigate the role of *CYC* in the expression of floral zygomorphy.

Acknowledgements

This study was supported by grants from a Grant-in-Aid for Scientific Research from the Ministry of Education, Culture, Sports Science and Technology (MEXT), Japan. We thank Dr. T. Fukuda for information on the primer sequences.

References

Baldwin, B., Kalisz, S., Armbruster, W.S., 2011. Phylogenetic perspectives on diversification, biogeography, and floral evolutions of *Collinsia* and *Tonella* (Plantaginaceae). Am. J. Bot. 98, 731−753.

Bartlett, M.E., Specht, C.D., 2011. Changes in expression pattern of the *TEOSINTE BRANCHED1*-like genes in Zingiberales provide a mechanism for evolutionary shifts in symmetry across the order. Am. J. Bot. 98, 227−243.

Chapman, M.A., Leebens-Mack, J.H., Burke, J.M., 2008. Positive selection and expression divergence following gene duplication in the sunflower CYCLOIDEA gene family. Mol. Biol. Evol. 25, 1260−1273.

Citerme, H., Jabbour, F., Nadot, S., Damerval, C., 2010. The evolution of floral symmetry. Adv. Bot. Res. 54, 85−137.

Citerne, H.L., Möller, M., Cronk, Q.C.B., 2000. Diversity of *cycloidea*-like genes in Gesneriaceae in relation to floral symmetry. Ann. Bot. 86, 167−176.

Citerne, H.L., Pennington, R.T., Cronk, Q.C.B., 2006. An apparent reversal in floral symmetry in the legume *Cadia* is a homeotic transformation. Proc. Natl. Acad. Sci. USA 103, 12017−1220.

Cubas, P., 2004. Floral zygomorphy, the recurring evolution of a successful trait. BioEssays 26, 1175−1184.

Cubas, P., Coen, E., Zapater, J.M., 2001. Ancient asymmetries in the evolution of flowers. Curr. Biol. 11, 1050−1052.

Cubas, P., Lauter, N., Doebley, J., Coen, E., 1999. The TCP domain: a motif found in proteins regulating plant growth and development. Plant J. 18, 215−222.

Galtier, N., Gouy, M., Gautier, C., 1996. SEAVIEW and PHYLO_WIN: two graphic tools for sequence alignment and molecular phylogeny. Comput. Appl. Biosci. 12, 543−548.

Doebley, J., Stec, A., Hubbard, L., 1997. The evolution of apical dominance in maize. Nature 386, 485−488.

Endress, P.K., 1999. Symmetry in flowers: diversity and evolution. Int. J. Plant Sci. 160, S3−S23.

Feng, X., Zhao, Z., Tian, Z., Xu, S., Luo, Y., Cai, Z., Wang, Y., Yang, J., Wang, Z., Weng, L., Chen, J., Zheng L., Guo, X., Luo J., Sato, S., Tabata, S., Ma, W., Cao, X., Hu, X., Sun, C., Luo, D., 2006. Control of petal shape and floral zygomorphy in *Lotus japonicus*. Proc. Natl. Acad. Sci. USA 103, 4970−4975.

Fukuda, T., Yokoyama, J., Maki, M., 2003. Molecular evolution of *cycloidea*-like genes in Fabaceae. J. Mol. Evol. 57, 588−597.

Hirai, M., Kamimura, T., Kanno, A., 2007. The expression patterns of three class B genes in two distinctive wholes of petaloid tepals in *Alstroemeria ligtu*. Plant Cell Physiol. 48, 310−321.

Hirai, M., Yamagishi, M., Kanno, A., 2012. Reduced transcription of a *LEAFY*-like gene in *Alstroemeria* sp. cultivar Green Coral that cannot develop floral meristems. Plant Sci. 185−186, 298−308.

Hofreiter, A., Rodriguez, E.F., 2006. The Alstroemeriaceae in Peru and neighbouring areas. Rev. Peruana de Biol. 13, 5−69.

Hoshino, Y., Kashihara, Y., Hirano, T., Murata, N., Shinoda, K., 2008. Plant regeneration from suspension cells induced from hypocotyls derived from interspecific cross *Alstroemeria pelegrina* × *A. magenta* and transformation with *Agrobacterium tumefaciens*. Plant Cell Tiss. Org. Cult. 94, 45–54.

Howarth, D.F., Donoghue, M.J., 2006. Phylogenetic analysis of the "ECE" (CYC/TB1) clade reveals duplications predating the core eudicots. Proc. Natl. Acad. Sci. USA 103, 9101−9106.

Howarth, D.G., Martins, T., Chimney, E., Donoghue, M.J., 2011. Diversification of *CYCLOIDEA* expression in the evolution of bilateral flower symmetry in Caprifoliaceae and *Lonicera* (Dipsacales). Ann. Bot. 107, 1521−1532.

Jabbour, F., Nadot, S., Damerval, C., 2009. Evolution of floral asymmetry: a state of the art. CR Biol. 332, 219−231.

Kashihara, Y., Shinoda, K., Murata, N., Araki, H., Hoshino, Y., 2011. Evaluation of the horticultural traits of genus *Alstroemeria* L. and genus *Bomarea* Mirb. (Alstroemeriaceae). Turk. J. Bot. 35, 239−245.

Kim, J.B., Raemakers, C.J.J.M., Jacobsen, E., Visser, R.G.F., 2007. Efficient production of transgenic *Alstroemeria* plants by using *Agrobacterium tumefaciens*. Ann. Appl. Biol. 151, 401−412.

Kobayashi, S., Saito, H., Okada, M., 1994. A simplified and efficient method for *in situ* hybridization to whole *Drosophila* embryos, using electrophoresis for removing non-hybridized probes. Dev. Growth Differ. 36, 629−632.

Kölsch, A., Gleissberg, S., 2006. Diversification of *CYCLOIDEA*-like TCP genes in the basal eudicot families Fumariaceae and Papaveraceae s.str. Plant Biol. 8, 680−687.

Kosugi, S., Ohashi, Y., 1997. PCF1 and PCF2 specifically bind to *cis* elements in the rice proliferating cell nuclear antigen gene. Plant Cell 9, 1607−1619.

Kosugi, S., Ohashi, Y., 2002. DNA binding and dimerization specificity and potential targets for the TCP protein family. Plant J. 30, 337−348.

Luo, D., Carpenter, R., Copsey, L., Vincent, C., Clark, J., Coen, E., 1999. Control of organ asymmetry in flowers of *Antirrhinum*. Cell 99, 367−376.

Luo, D., Carpenter, R., Vincent, C., Copsey, L., Coen, E., 1996. Origin of floral asymmetry in *Antirrhinum*. Nature 383, 794−799.

Martín-Trillo, M., Cubas, P., 2010. TCP gens: a family snapshot ten years later. Trends Plant Sci. 15, 31−39.

Mondragón-Palomino, M., Trontin, C., 2011. High time for a roll call: gene duplication and phylogenetic relationships of TCP-like genes in monocots. Ann. Bot. 107, 1533−1544.

Preston, J., Hileman, L.C., 2009. Development of genetics of floral symmetry evolution. Trends Plant Sci. 14, 147−154.

Preston, J., Hileman, L.C., 2012. Parallel evolution of TCP and B-class genes in Commelinaceae flower bilateral symmetry. EvoDevo 3, 6.

Reeves, P.A., Olmstead, R.G., 2003. Evolution of the TCP gene family in Asteridae: cladistic and network approaches to understanding regulatory gene family diversification and its impact on morphological evolution. Mol. Biol. Evol. 20, 1997−2009.

Rudall, P.J., Bateman, R.M., 2004. Evolution of zygomorphy in monocot flowers: iteractive patterns and developmental constraints. New Phytol. 162, 25−44.

Stebbins, G.L., 1974. Flowering Plants: Evolution Above the Species Level. Washington, DC: Harvard University Press.

Vieira, C.P., Vieira, J., Charlesworth, D., 1999. Evolution of the cycloidea gene family in *Antirrhinum* and *Misopates*. Mol. Biol. Evol. 16, 1474−1483.

Wang, Z., Luo, Y., Li, X., Wang, L., Xu, S., Yang J, Weng, L., Sato, S., Tabata, S., Ambrose, M., Rameau, C., Feng, X., Hu, X., Luo, D., 2008. Genetic control of

floral zygomorphy in pea (*Pisum sativum* L.). Proc. Natl. Acad. Sci. USA;105, 10414−10419.

Yuan, Z., Gao, S., Xue, D.W., Luo, D., Li, L.T., Ding, S.Y., Yao, X, Wilson Z.A., Qian Q., Zhang D.B., 2009. *RETARDED PALEA1* controls palea development and floral zygomorphy in rice. Plant Physiol. 149, 235−244.

Figure legends

Figure 1. *Alstroemeria* spp. used in the present study and floral zygomorphy in *Alstroemeria*. (a) Plants of *A. pelegrina* var. *rosea* at the flowering stage (scale = 10 cm); (b) flower of *A. pelegrina* var. *rosea* (scale = 3 cm); (c) flower of *A. aurea* (scale = 3 cm); (d) flower of *A. magenta* (scale = 3 cm). (e) A representative *Alstroemeria* flower showing floral zygomorphy. Black straight line indicates a symmetrical axis. Specific spots are observed on 2 perianths enclosed with curve lines.

Figure 2. Conserved amino acid sequences of the TCP and R domains in *CYC* homologue genes of *Alstroemeria* spp. and reference species. Deduced amino acid sequences of *AaTCP1*, *ApTCP2*, *ApTCP1*, and *AmTCP1* were aligned with *CYCLOIDEA* (accession number Y16313), *DICHOTOMA* (AF199465), *TB1* (U94494), *OsTB1* (AB088343), and *TCP1* (AC002130).

Figure 3. Molecular phylogenetic analysis of amino acid sequences of TCP domain in *CYC*-like genes using the maximum likelihood (ML) method. Numerals indicate bootstrap values from 100 replicates. The abbreviations of gene names and GenBank/EMBL/DDBJ database accession numbers are as follows: OsTCP6 (*Oryza sativa TCP6*; GQ229483), AtTCP8 (*Arabidopsis thaliana TCP8*; NM_001084270), SlTCP11 (*Solanum lycopersicum TCP11*; NM_001247902), AtTCP6 (*Arabidopsis thaliana TCP6*; NM_123468), ZmTCP-domain (*Zea mays TCP-domain protein*; NM_001158303), AtTCP9 (*Arabidopsis thaliana TCP9*; NM_130131), AtTCP7 (*Arabidopsis thaliana TCP7*; NM_122234), AtTCP3 (*Arabidopsis thaliana TCP3*; AF072134), AtTCP4 (*Arabidopsis thaliana TCP4*; NM_180258), SlCycloidea (*Solanum lycopersicum Cycloidea*; NM_001247406),

SlTCP3-1 (*Solanum lycopersicum TCP3*; NM_001247438), SlTCP10 (*Solanum lycopersicum TCP10*; NM_001247647), SlTCP1-2 (*Solanum lycopersicum TCP1*; NM_001246854), ZmTCPfam (*Zea mays TCP family transcription factor*; NM_001157836), OsTCP11 (*Oryza sativa TCP11*; GQ229484), SlTCP5 (*Solanum lycopersicum TCP5*; NM_001246863), AtTCP5 (*Arabidopsis thaliana TCP5*; NM_125490), SlTCP4 (*Solanum lycopersicum TCP4*; NM_001247635), SlTCP6 (*Solanum lycopersicum TCP6*; NM_001247639), AtTCP2 (*Arabidopsis thaliana TCP2*; AF072691), PaTB1-TCP (*Plagiostachys albiflora TB1-TCP*; HM775146.1), PmTB1-TCP (*Plagiostachys mucida TB1-TCP*; HM775147.1), PmTCP1 (*Plantago major TCP1*; AY168138), AmTCP4 (*Antirrhinum majus TCP4*; AY168143), AmTCP3 (*Antirrhinum majus TCP3*; AY168142), AmDICHOTOMA (*Antirrhinum majus DICHOTOMA*; AF199465), AtTCP1 (*Arabidopsis thaliana TCP1*; NM_001160982), AmTCP2 (*Antirrhinum majus TCP2*; AY168141), AmCycloidea (*Antirrhinum majus Cycloidea*; Yl6313), LoTCP1 (*Ligustrum ovalifolium TCP1*; AY168156), SlTCP2 (*Solanum lycopersicum TCP2*; AY168166), SlTCP7 (*Solanum lycopersicum TCP7*; NM_001246868), SpTCP7 (*Schizanthus pinnatus* TCP7; AY168174), SpTCP5 (*Schizanthus pinnatus TCP5*; AY168172), SpTCP6 (*Schizanthus pinnatus TCP6*; AY168173), PmTCP2 (*Plantago major TCP2*; AY168139), CtTCP1 (*Calceolaria tenella TCP1*; AY168152), CtTCP2 (*Calceolaria tenella TCP2*; AY168153), LoTCP3 (*Ligustrum ovalifolium TCP3*; AY168158), AmTCP1 (*Antirrhinum majus TCP1*; AY168140), SpTCP3 (*Schizanthus pinnatus TCP3*; AY168170), SpTCP4 (*Schizanthus pinnatus TCP4*; AY168171), EpTCP1 (*Echium plantagineum TCP1*; AY168175), SlTCP1 (*Solanum lycopersicum TCP1*; AY168165), NsTCP1 (*Nicotiana sylvestris TCP1*; AY168163), AcTBLb (*Acorus calamus TBLb*; HM775145.1), AcTBLa (*Acorus calamus TBLa*; HM775144.1),

LoTCP2 (*Ligustrum ovalifolium TCP2*; AY168157), AmTCP5 (*Antirrhinum majus TCP5*; AY168144.1), SpTCP2 (*Schizanthus pinnatus TCP2*; AY168169), NsTCP2 (*Nicotiana sylvestris TCP2*; AY168164), SlTCP9 (*Solanum lycopersicum TCP9*; GQ496327), AtBRANCHED1 (*Arabidopsis thaliana BRANCHED1*; AM408560), ZmTCPtrans (*Zea mays TCP transcription factor*; NM_001136610), OsDP1 (*Oryza sativa DP1*; EU702407), CcTBL2b (*Calathea crotalifera TBL2b*; HM775133.1), AvTBL2 (*Alpinia vittata TBL2*; HM775135.1), ZoTBL2b2 (*Zingiber ottensii TBL2b.2*; HM775138.1), ZoTBL2 (*Zingiber officinale TBL2*; HM775136.1), ZoTBL2b1 (*Zingiber ottensii TBL2b.1*; HM775137.1), GlTBL2b (*Globba laeta TBL2b*; HM775134.1), CcTBL2a (*Calathea crotalifera TBL2a*; HM775131.1), HcTBL2 (*Heliconia chartacea* TBL2; HM775126), HpTBL2 (*Heliconia pendula TBL2*; HM775128), HsTBL2 (*Heliconia stricta TBL2*; HM775132), CaTBL2 (*Costus amazonicus TBL2*; HM775124.1), SnTBL2 (*Strelitzia nicolai voucher TBL2*; HM775127.1), GlTBL2a (*Globba laeta TBL2a*; HM775129.1), SlTCP3 (*Solanum lycopersicum TCP3*; AY168167), SlTCP8 (*Solanum lycopersicum TCP8*; NM_001247643), SpTCP1 (*Schizanthus pinnatus TCP1*; AY168168), AlstpelTCP2 (ApTCP2) (*Alstroemeria pelegrina TCP2*; AB714969), LlTCP1 (*Lilium longiflorum TCP1*; EF095959.1), OmTBL1a (*Orchidantha maxillarioides TBL1a*; HM775093), HsTBL1a (*Heliconia stricta TBL1a*; HM775094), AvTBL1a (*Alpinia vittata TBL1a*; HM775103.1), CcTBL1a (*Calathea crotalifera TBL1a*; HM775096.1), CrTBL1a (*Curcuma rubrobracteata TBL1a*; HM775098), RlTBL1a (*Riedelia lanata TBL1a*; HM775099.1), SnTBL1a (*Strelitzia nicolai voucbher TBL1a*; HM775102.1), MuTBL1a (*Monocostus uniflorus TBL1a*; HM775101.1), PhTBL1a (*Pleuranthodium hellwigii TBL1a*; HM775097.1), AlstauTCP1 (AaTCP1) (*Alstroemeria aurea TCP1*; AB714967), AlstpelTCP1 (ApTCP1) (*Alstroemeria pelegrina TCP1*; AB714968),

AlstmagTCP1 (AmTCP1) (*Alstroemeria magenta TCP1*; AB714970), CrTBL1b (*Curcuma rubrobracteata TBL1b*; HM775107.1), EcTBL1b (*Elettaria cardamomum TBL1b*; HM775113.1), BnTBL1b (*Burbidgea nitida TBL1b*; HM775110.1), AvTBL1b (*Alpinia vittata TBL1b*; HM775112.1), EuTBL1b (*Elettariopsis unifolia TBL1b*; HM775111.1), RlTBL1b (*Riedelia lanata TBL1b*; HM775108.1), PhTBL1b (*Pleuranthodium hellwigii TBL1b*; HM775109.1), CcTBL1b (*Calathea crotalifera TBL1b*; HM775118.1), CsTBL1b (*Costus spicatus TBL1b*; HM775115.1), CaTBL1b (*Costus amazonicus TBL1b*; HM775114.1), HsTBL1b (*Heliconia stricta TBL1b*; HM775117), CspTBL21 (*Canna sp. TBL2.1*; HM775105.1), CspTBL22 (*Canna sp. TBL2.2*; HM775104.1), MbTBL1b (*Musa basjoo TBL1b*; HM775142.1), SrTBL1b (*Strelitzia reginae TBL1b*; HM775120.1), SnTBL1b (*Strelitzia nicolai TBL1b*; HM775121.1), MlTBL1b (*Maranta leuconeura* TBL1b; HM775116.1), OsTB1 (*Oryza sativa TB1*; AB088343), PaTB1 (*Pleioblastus amarus* TB1; DQ910764.1), YnTB1 (*Yushania niitakayamensis* TB1; DQ910763.1), HvTCP (*Hordeum vulgare* TCP; JF904738.1), ZmTB1 (*Zea mays TB*; U94494), PgTB1 (*Pennisetum glaucum Tb1*; EF694127.2), PdTB1 (*Phacelurus digitatus TB1*; AF322125), SbTB1 (*Sorghum bicolor TB1*; AF322132), and AgTB1 (*Andropogon gerardii TB1*; AF322119).

Figure 4. RT-PCR analysis of *AaTCP1* transcripts in flower buds (FB), leaves (L), and stems (S) of *Alstroemeria aurea*. The number of PCR cycles was 35. The actin gene was used as the internal control.

Figure 5. RT-PCR analysis of *AaTCP1* transcripts in *Alstroemeria aurea* flower buds of different developmental stages. Quantitative RT-PCR, conducted by

altering the number of PCR cycles for flower buds of 0.5−1, 1−2, and 2−3 mm in length and using the actin gene as the internal control.

Figure 6. Localization of *AaTCP1* transcripts detected using *in situ* hybridization of flower buds of *Alstroemeria aurea*. Flower buds of 3 mm longitudinal diameter were used to prepare transverse serial sections of 10 μm thickness. (a) *In situ* hybridization using DIG-labelled antisense *AaTCP1* probe. (b) *In situ* hybridization using DIG-labelled sense *AaTCP1* probe. ip, inner perianth; op, outer perianth; fi, filament; g, gynoecium. Scale = 500 μm.

Figure 7. Localization of AaTCP1 transcripts in longitudinal sections detected using in situ hybridization of *Alstroemeria aurea*. Flower buds of 3 mm longitudinal diameter were used to prepare serial sections of 10 μm thickness. (a) *In situ* hybridization using DIG-labelled antisense *AaTCP1* probe. (b) *In situ* hybridization using DIG-labelled sense *AaTCP1* probe. an, anther; ip, inner perianth; op, outer perianth; fi, filament. Scale = 500 μm.

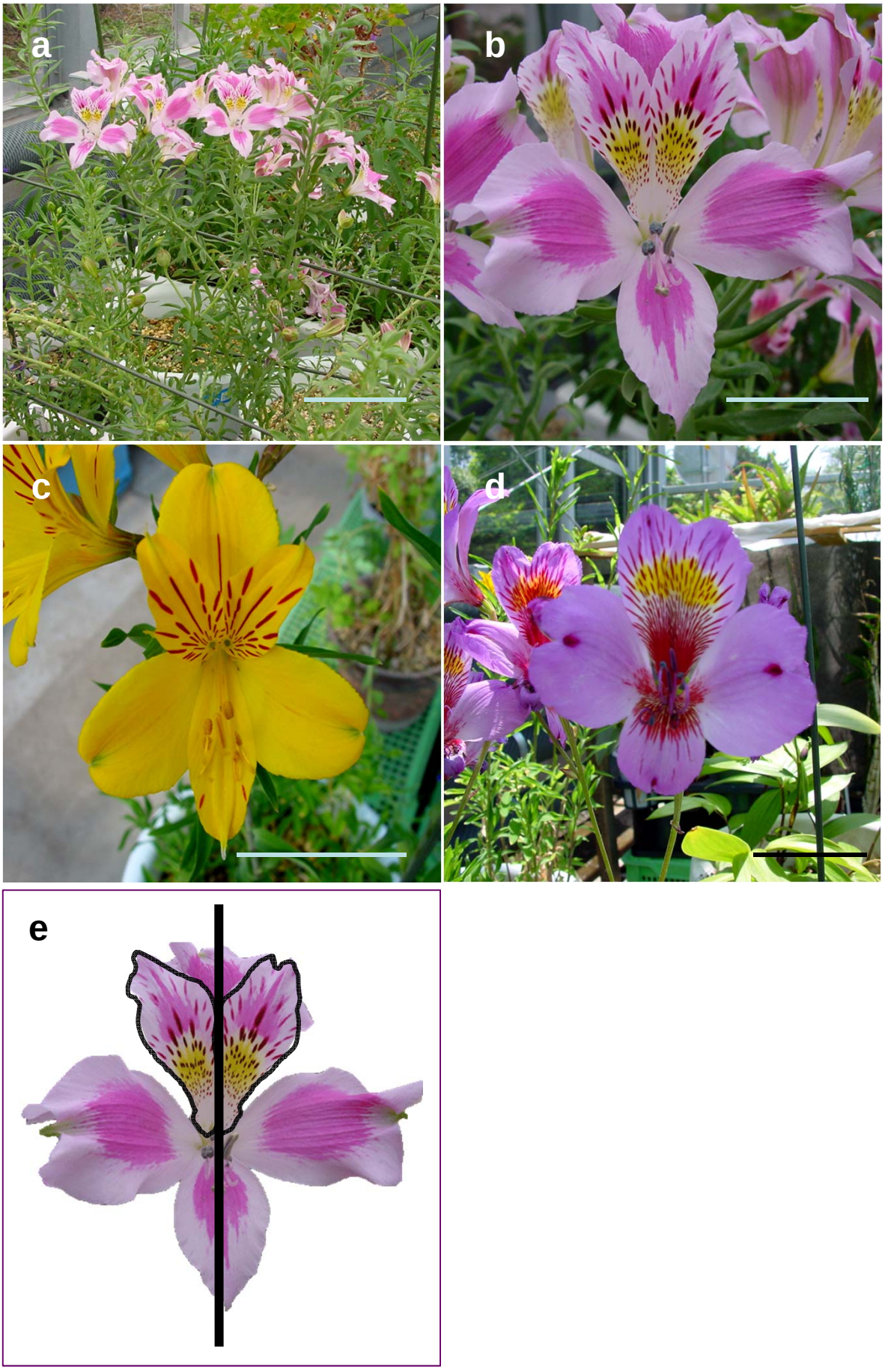

Figure 1

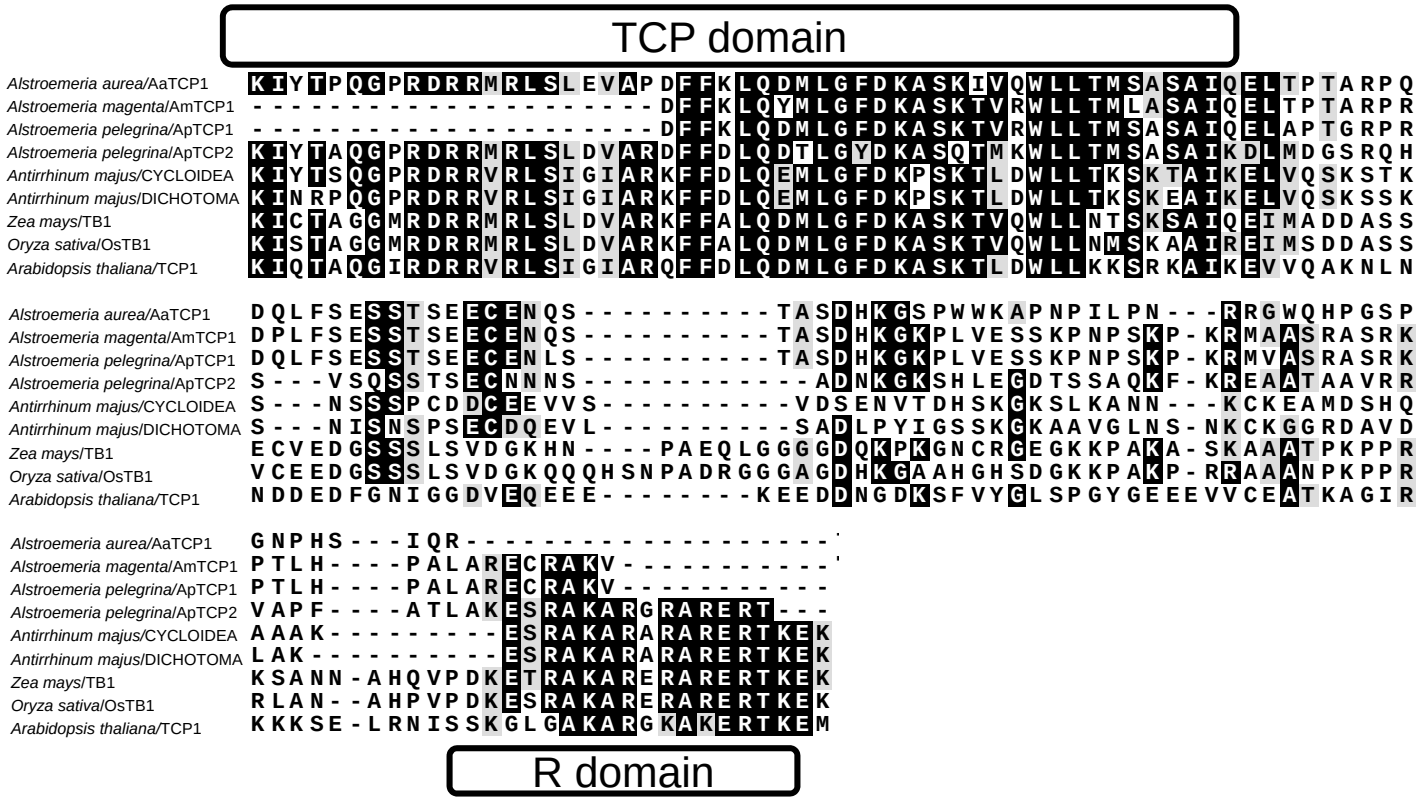
TCP domain
Alstroemeria aurea/AaTCP1 KIYTPQGPRDRRMRLSLEVAPDFFKLQDMLGFDKASKIVQWLLTMSASAIQELTPTARPQ
Alstroemeria magenta/AmTCP1 ----------DFFKLQYMLGFDKASKTVRWLLTMLASAIQELTPTARPR
Alstroemeria pelegrina/ApTCP1 ----------DFFKLQDMLGFDKASKTVRWLLTMSASAIQELAPTGRPR
Alstroemeria pelegrina/ApTCP2 KIYTAQGPRDRRMRLSLDVARDFFDLQDTLGYDKASQTMKWLLTMSASAIKDLMDGSRQH
Antirrhinum majus/CYCLOIDEA KIYTSQGPRDRRVRLSIGIARKFFDLQEMLGFDKPSKTLDWLLTKSKTAIKELVQSKSTK
Antirrhinum majus/DICHOTOMA KINRPQGPRDRRVRLSIGIARKFFDLQEMLGFDKPSKTLDWLLTKSKEAIKELVQSKSSK
Zea mays/TB1 KICTAGGMRDRRMRLSLDVARKFFALQDMLGFDKASKTVQWLLNTSKSAIQEIMADDASS
Oryza sativa/OsTB1 KISTAGGMRDRRMRLSLDVARKFFALQDMLGFDKASKTVQWLLNMSKAAIREIMSDDASS
Arabidopsis thaliana/TCP1 KIQTAQGIRDRRVRLSIGIARQFFDLQDMLGFDKASKTLDWLLKKSRKAIKEVVQAKNLN
Alstroemeria aurea/AaTCP1 DQLFSESSTSEECENQS----------TASDHKGSPWWKAPNPILPN---RRGWQHPGSP
Alstroemeria magenta/AmTCP1 DPLFSESSTSEECENQS----------TASDHKGKPLVESSKPNPSKP-KRMAASRASRK
Alstroemeria pelegrina/ApTCP1 DQLFSESSTSEECENLS----------TASDHKGKPLVESSKPNPSKP-KRMVASRASRK
Alstroemeria pelegrina/ApTCP2 S---VSQSSTSECNNNS----------ADNKGKSHLEGDTSSAQKF-KREAATAAVRR
Antirrhinum majus/CYCLOIDEA S---NSSSPCDDCEEVVS----------VDSENVTDHSKGKSLKANN---KCKEAMDSHQ
Antirrhinum majus/DICHOTOMA S---NISNSPSECDQEVL----------SADLPYIGSSKGKAAVGLNS-NKCKGGRDAVD
Zea mays/TB1 ECVEDGSSSLSVDGKHN----PAEQLGGGGDQKPKGNCRGEGKKPAKA-SKAAATPKPPR
Oryza sativa/OsTB1 VCEEDGSSSLSVDGKQQQHSNPADRGGGAGDHKGAAHGHSDGKKPAKP-RRAAANPKPPR
Arabidopsis thaliana/TCP1 NDDEDFGNIGGDVEQEEE--------KEEDDNGDKSFVYGLSPGYGEEEVVCEATKAGIR
Alstroemeria aurea/AaTCP1 GNPHS---IQR----------
Alstroemeria magenta/AmTCP1 PTLH----PALARECRAKV----------
Alstroemeria pelegrina/ApTCP1 PTLH----PALARECRAKV----------
Alstroemeria pelegrina/ApTCP2 VAPF----ATLAKESRAKARGRARERT---
Antirrhinum majus/CYCLOIDEA AAAK----------ESRAKARARARERTKEK
Antirrhinum majus/DICHOTOMA LAK----------ESRAKARARARERTKEK
Zea mays/TB1 KSANN-AHQVPDKETRAKARERARERTKEK
Oryza sativa/OsTB1 RLAN--AHPVPDKESRAKARERARERTKEK
Arabidopsis thaliana/TCP1 KKKSE-LRNISSKGLGAKARGKAKERTKEM
R domain

Figure 2

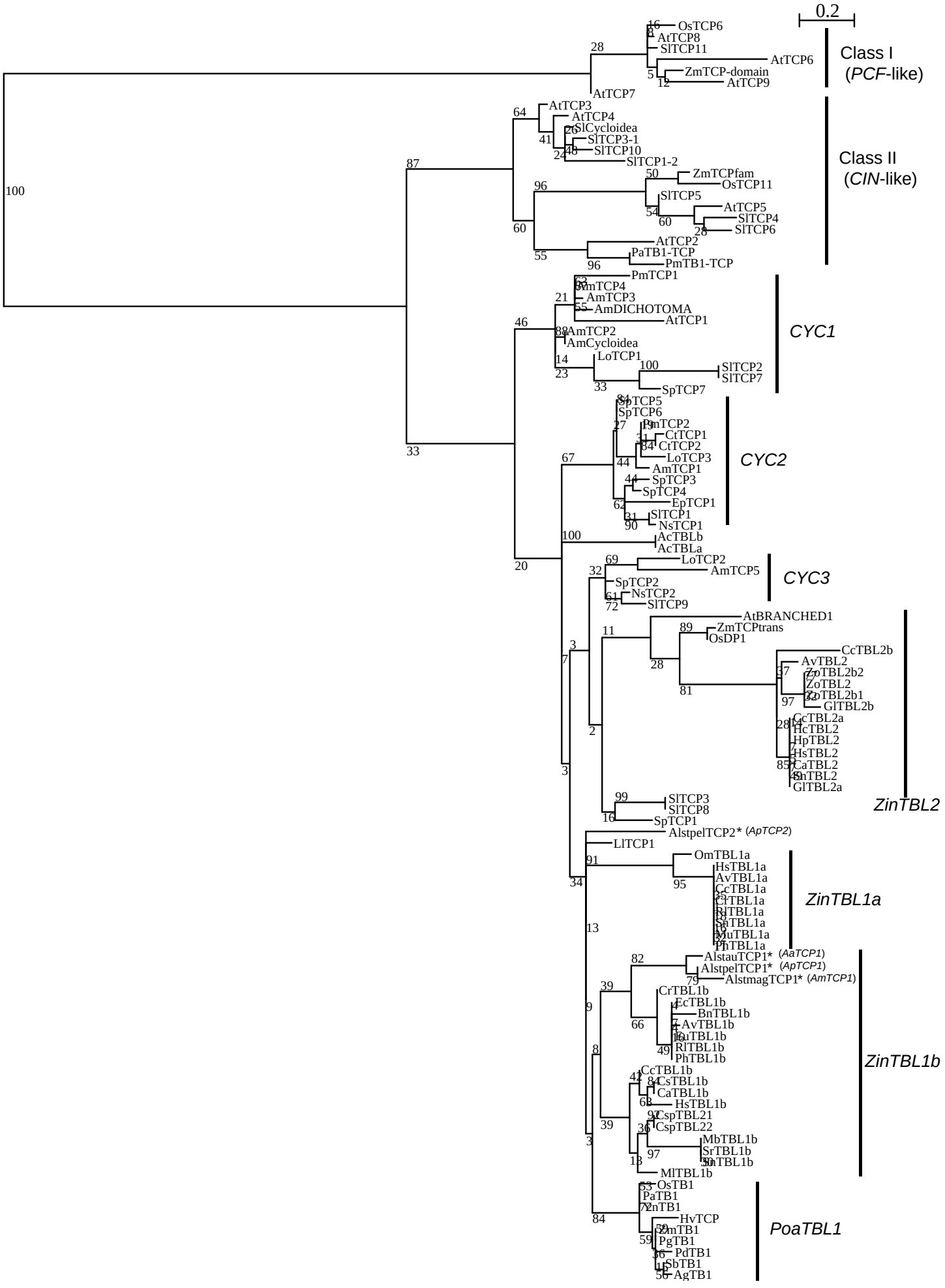

Figure 3

* This study

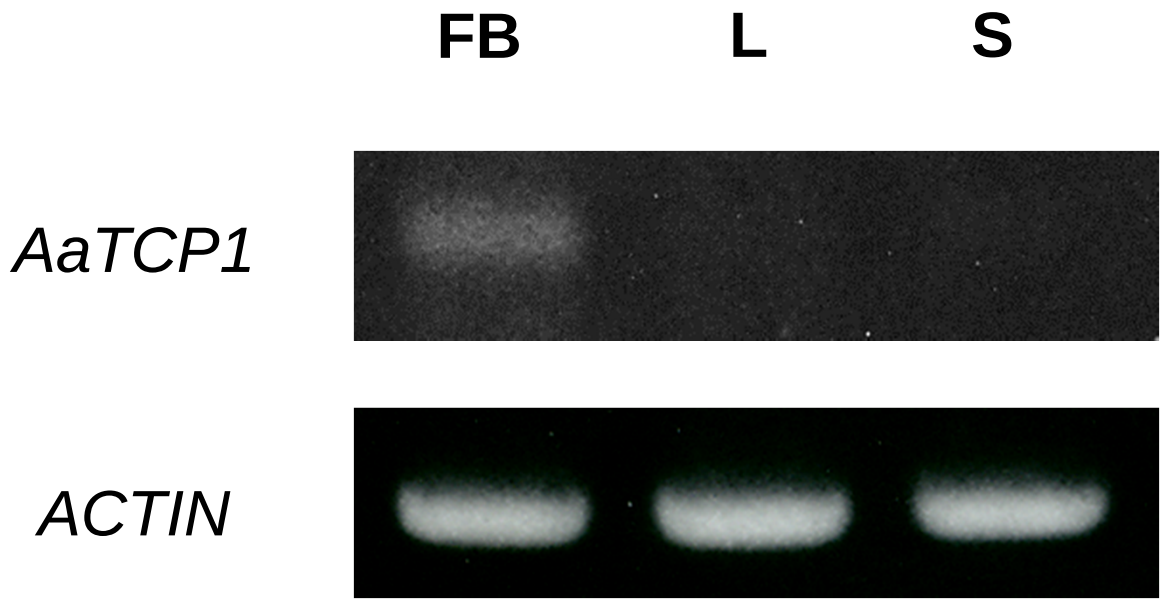

Figure 4

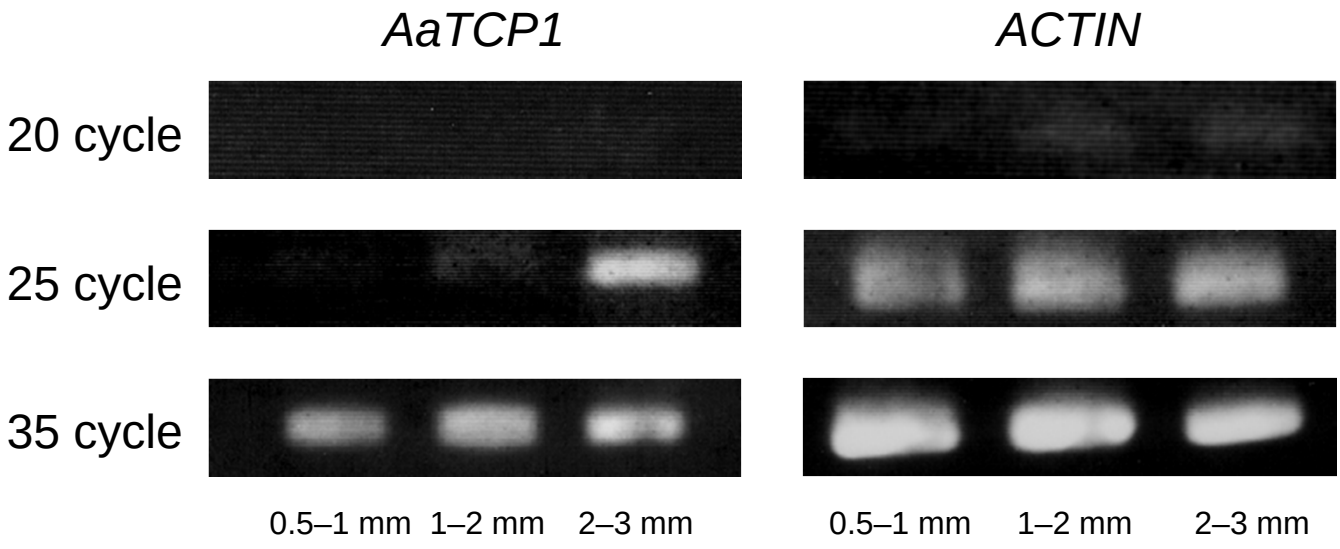
AaTCP1
ACTIN
20 cycle
25 cycle
35 cycle
0.5–1 mm
1–2 mm
2–3 mm
0.5–1 mm
1–2 mm
2–3 mm

Figure 5

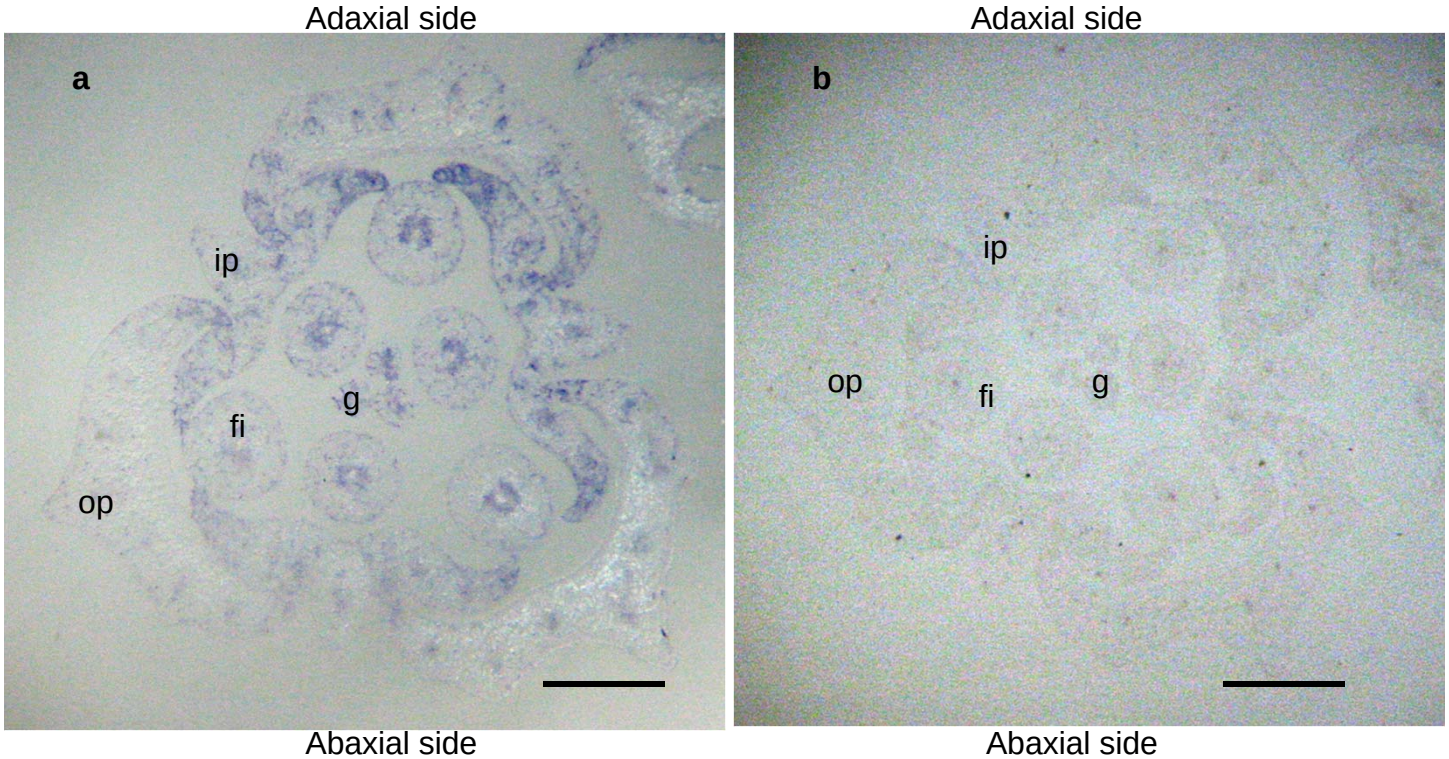
Adaxial side
Adaxial side
a
b
ip
ip
op
fi
g
op
fi
g
Abaxial side
Abaxial side

Figure 6

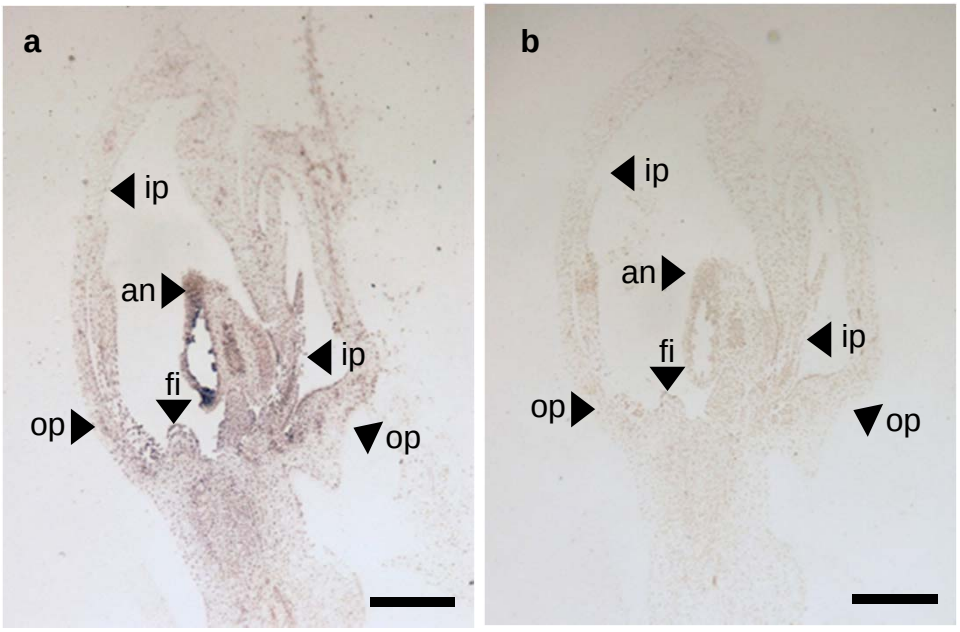

Figure 7